International Journal of Science and Research Archive
eISSN: 2582-8185
Cross Ref DOI: 10.30574/ijsra
Journal homepage: https://ijsra.net/

(RESEARCH ARTICLE)

An Electrochemical Impedance Spectroscope (EIS) investigation on the influence of acetic acid on corrosion of mild steel

Ikeh Lesor * and Ebeze Peter Anene

Department of Petroleum and Gas Engineering, Faculty of Engineering, University of Port Harcourt, East–West Road, Choba, Uniport.

International Journal of Science and Research Archive, 2026, 19(01), 534-549

Publication history: Received on 03 March 2026; revised on 09 April 2026; accepted on 11 April 2026

Article DOI: https://doi.org/10.30574/ijsra.2026.19.1.0755

Abstract

Corrosion affects pipelines and their operation. If corrosion remains undetected or unmanaged, it will cause metal loss, leading to costly repair downtime. Severe corrosion, if left untreated, could lead to catastrophic pipeline failure, resulting in major equipment damage, environmental damage, safety incidents, and even loss of life. Several studies have shown that corrosion products (ferrous and anhydrous ions) combine to form porous, non-protective precipitates on iron surfaces. To prevent these issues, Mono-Ethylene Glycol (MEG) is used in pipelines as an antifreeze and anti-corrosion agent. It is important to note that MEG must be separated from acetic acid (HAc) and acid gases, which can accelerate corrosion of mild steel in oil-field environments. Additionally, mono-ethylene glycol and acetic acid can decrease the solubility of mineral salts, thereby increasing the risk of corrosion. The study aims to investigate the effects of acetic acid and mono-ethylene glycol on the corrosion rate of mild steel in saturated brine solutions at different temperatures. Electrochemical measurements using an Electrochemical Impedance Spectroscopy (EIS) instrument were employed to measure the corrosion rate as a function of time at different HAc and MEG concentrations. Furthermore, the efficiencies of three corrosion-inhibiting chemicals, the phosphate ester and the oleic imidazoline salt at various concentrations, were evaluated. The EIS results show that the corrosion rate in the presence of HAc increases with increasing HAc concentration and decreases with increasing exposure time due to the protective film formed on the electrode surface. The Nyquist and Bode plots of the EIS results indicate that the diameter of the depressed semicircle decreases as various concentrations of HAc and MEG are added to the solution, and the and the sizes of the capacitive semicircle also decrease upon addition of 20% and 80% MEG.This reduction in corrosion rate is attributed to the formation of an iron carbonate film on the surface of the steel sample.

Keywords: Corrosion; Acetic Acid; Mild Steel; EIS; MEG; Iron Carbonate; Film

1. Introduction

In recent years, there have been several national studies on the costs of corrosion covering a range of countries including the United States of America and the United Kingdom (Charng et al, 1982). The impact of corrosion on the oil and gas industry has been examined in terms of its effects on capital expenditure (CAPEX), operational expenditures (OPEX), and health, safety, and environment (HSE) (Chechirlian et al., 1990). However, the direct costs of corrosion-related degradation are estimated to be around 3-4% of the Gross Domestic Product (GDP) in industrial countries. Kermani and Harrop proposed that the corrosion of metallic structures poses a significant threat to a company's economy. Kosh et al in their studies presents a summary of data from the USA where a detailed analysis has been performed to estimate costs at about 276 billion dollars per year which correspond to about 3.1% of the gross domestic product (GDP). These costs were determined by analyzing 26 industrial sectors known to be affected by corrosion and include the costs of design, manufacturing, construction and management.

* Corresponding author: Ikeh Lesor

1.1. Assessment of corrosion failure in industry

Corrosion can impose a significant cost on material selection during design stage, and its potential occurrence also carriers' serious safety and environmental risks. A corrosion failure can severely impact the environment. In the offshore oil industry, leaks from subsea oil well tubulars, transmission pipelines, storage vessels, and other equipment on offshore platforms threaten pollution of the sea. When it comes directly from the well, the fluid is typically unprocessed and multiphase, often a mixture of oil, solids, gas, and water. The presence of water causes significant corrosion problems on the internal walls of pipelines. The liquid may contain corrosive species such as organic acids and dissolved gases like such as carbon dioxide (CO_2) or hydrogen sulphide (H_2S). Thus, these gases can create highly corrosive environments. Carbon dioxide (CO_2) corrosion, also known as sweet corrosion, has been a long-standing issue and continues to be a costly problem in the oil and gas industry, costing billions annually. CO_2 exists in the oil phase with water as a dissolved gas under the high pressures commonly found in underground reservoirs. In its dissolved form, it creates, carbonic acid.

$$CO_2 + H_2O \leftrightarrow H_2CO_3 \quad (1)$$

The pipeline costs are a significant part of the investment in subsea projects. For long-distance, large-diameter pipelines, they can become prohibitively high if the corrosiveness of the fluid requiires the use of corrosion-resistant alloys instead of carbon steel. Therefore, better understanding and control of the corrosion of carbon steel can expand its application range and have a substantial economic impact.

Carbon steel is used as the primary construction material for pipelines in the oil and gas industry because of its low cost and availability. However, it is highly susceptible to corrosion in CO_2 environments. Carbon dioxide corrosion has long concerned many researchers in the oil and gas industry, and numerous theories have been proposed regarding its mechanism (Dugstad, 1988). Similarly, there has been significant interest in understanding how different factors affect the mechanism of CO_2 corrosion and the formation of iron carbonate film on the surface of carbon steel due to its impacts on the corrosion rate.

Acetic acids (HAc) are considered sources of hydrogen ions during dissociation, which increase environmental acidity and promote the dissolution of steel that leading to higher corrosion rates of carbon steel, especially at low pH levels. Acetic acid is the most common organic acid in multiphase systems containing brine. Its concentrations in oil wells significantly influences corrosion severity, even when present in small amounts. The precipitation of iron carbonate ($FeCO_3$) is a key process for controlling corrosion in the oil industry. The formed FeCO3 layer creates an impermeable film that slows down corrosion by diffusion control. This protective layer plays a vital role in reducing corrosion rates. Without deposition of corrosion products on the steel surface, corrosion rate can reach several millimeters per year. The rate can be substantially lowered when $FeCO_3$ precipitates on the steel, creating a dense, protective film. This process is more easily facilitated at high temperatures or high pH levels in the water phase. When hydrogen sulphide (H_2S) is also present along with CO2, iron sulphide (FeS) films form instead of $FeCO_3$, allowing protective films to develop at lower temperatures.

Corrosion inhibitors are of the many methods used to protect against corrosion in the oil and gas industry. These inhibitors are commonly used to slow down the corrosion process of mild steel in oilfield environments. They can reduce metalcorrosion by forming a protective film that isolates the metal from the aqueous corrosion environment. Water-soluble and oil-soluble inhibitors are the most commonly used in the oil and gas industry.

The mechanism of CO_2 corrosion and the kinetics of formating and removing $FeCO_3$ film are not fully understood because complex complex reaction mechanisms, and the influence of many environmental factors such as pH, temperature, dissolved species concentrations, and hydrodynamics that can alter the corrosion rate. This work aims to investigate the effect of HAc on mild corrosion using the potentiodynamic polarization resistance corrosion rate.

2. Acetic acid corrosion of carbon steel in CO_2 environment

Internal corrosion of pipelines constitutes a significant problem to the petroleum industry. CO_2 corrosion in the presence of HAc is known as a major reason for premature failures in oil and gas pipelines which are usually made of carbon steel. Crolet et al [41] reported that the presence of acetic acid in a saturated aqueous solution with CO_2 increases the corrosion rate from 1.3 to 5.7 mm/yr in the North Sea.Water and acidic gases such as carbon dioxide (CO_2), hydrogen sulphide (H_2S) and organic acids co-produced with the hydrocarbon constitute the corrosive environment. Carbon steel is presently the only economically feasible material for such pipelines, and the corrosion rates may reach about 10 mm/yr or more in the absence of mitigation measure like injection of corrosion inhibitors.

The presence of acetic acids (HAc) in oil and gas wells has been known since 1944 and its presence is frequent in oilfields when CO_2 is observe. Acetic acid is the most common organic acid in multiphase systems containing brine. The effect of acetic acid (HAc) on the corrosion rate of carbon steel in most oil and gas fields containing brine and CO_2 has been studied. It has been shown that acetic acids served as a corrosive agent in CO_2 corrosion. Nafday et al. and Garsany et al. have demonstrated that the presence of acetic acids decreases the protectiveness of iron carbonate films and this occur as a result of reduction in pH and a scale undermining effect. In oilfield pipelines with low ρCO_2, the corrosion issues are easily managed, but when small amounts of acetic acids are present, the corrosivity of the brine can change dramatically. It has been shown that the total quantity of organic acids in produced water in oil and gas system varies between 500-3000 ppm of which HAc contributes about 50-90% of organic acids. Similarly, a systematic investigation of field data showed that undissociated HAc concentration higher than 0.1-1 mM was a critical factor for CO_2 corrosion

Many studies have found that acetic acid's main role is that of a corrosion promoter and also as a corrosion inhibitor (Cottis, R.A. 2009, George et al, 2007). They conclude that the acetic acids may behave as corrosion inhibitors when the acids are absorbed on the metallic surface, acting as a barrier between the metal and the environment. Furthermore, Crolet et al. (1992), determined the effect of acetic acid on the cathodic and anodic charge transfer mechanisms in the presence of CO_2. They first studied the effect of acetic acid on potential sweeps at different pH levels and CO_2 partial pressures. It was found that the presence of acetic acid does not affect the cathodic limiting current density but inhibits the anodic charge-transfer mechanism. Though, the acetate ions have a limited effect on the pH because of the buffering action, they can play a significant role in the hydrogen evolution reaction which is a rate controlling step in the corrosion reaction. Hedges and McVeigh (2004) tested the effect of HAc on CO_2 corrosion at 60 □, 0.8 bar CO_2 partial pressure, 3% NaCl and synthetic formation water. It was found that the corrosion rates increased with increasing HAc concentration, and further increased again when more HAc was added to the cell. Nafday and Nesic studied the effect of HAc on $FeCO_3$ corrosion product film protectiveness at 80 □ in 3% wt NaCl and CO_2 partial pressure of 0.5 bars. The tests were carried out at relative $FeCO_3$ supersaturations of 32 and 162. It was found that no significant effect of HAc on $FeCO_3$ layer protectiveness or morphology was found in any of the tests. Ueda and Takabe later investigated the effect of 0.5% (5000ppm) HAc on carbon and chromium bearing steels at 60-300°C using autoclave tests at 30 bar CO_2 partial pressure, and 5% NaCl. They found that the corrosion rate was considerably higher with HAc than with only CO_2. It was also observed that the corrosion rate is lower at 60 □ where HAc related to the anodic inhibition. Liu et al (2001) studied the effect of HAc using electrochemical impedance spectroscopy (EIS). They found that the surface chemical reactions of cathodic reduction were enhanced in the presence of HAc. Furthermore, they found that HAc can remove $FeCO_3$ layer. Zhang and Cheng (2009) reported similar results, observing increased current density of anodic reactions and localized corrosion on the steel surface.

Dugstad et al (1995) tested the effect of 12 ppm undissociated HAc under film forming conditions at 80 □ using flow loop at CO_2 partial pressure of 2 bar, pH of 5.8, 0.1 % NaCl and supersaturation of 6-30ppm of Fe^{2+}. It was found that though, the corrosion attack varied considerably between the different steels tested, the HAc caused more mesa attack on the steel surfaces. The corrosion films were more fragmented, with more pores and flaws, and the localized corrosion was more severe at high rates. Singer et al. studied top-of-line (TOL) corrosion in presence of HAc and CO_2 at 70 □, 0-1000ppm HAc. It was observed that the corrosion rate in TOL increased gradually with increasing HAc concentration and with increasing condensation rates, and the rates were gradually lower than in the bottom of the line. Furthermore, Mendez et al (2010) extended the work of Singer et al. to include the effect of glycol and pH control. It was found that little effect of HAc was seen on the TOL corrosion rate after 2 to 3 days exposure. Oblonsky et al. (1998) found out that solid Fe_3O_4 and dissolved Fe^{2+} as the corrosion products in the corrosion of Fe in the solution saturated with argon, and in the presence of acetate ion. They found that acetate concentration had no effect on the chemical analysis of the corrosion product layer. Sun et al. (1988) used a rotating cylinder electrode with glass cell bubble tests to investigate the effect of HAc on the part reactions under N_2 and CO_2 atmospheric pressure and room temperature, HAc concentrations of 0-1000 ppm and 3 wt.-% NaCl. From the results obtained, it was showed that the HAc increased the cathodic current, and that the H_2 evolution from HAc was activation controlled at room temperature.

George et al. (2007) basically used Sun to further study the effect of HAc on the corrosion rate in the temperature range of 22-60 C, 0-1000ppm HAc concentration and 3 wt. % NaCl, and developed an electrochemical/hydrodynamic model for the cathodic reaction taking into account the reduction of H^+, H_2CO_3 and HAc from the bulk of the solution. It was observed that the cathodic current in presence of HAc was reduced in synthetic brine with high salt contents compared to 3 wt. % NaCl. The mass loss data showed no significant difference between them.

Okafor and Nesic (2009) reported that acetic acid can caused localized corrosion by removing iron carbonate layer. Similarly, George and Nesic reported that the presence of HAc strongly affects the cathodic limiting current. The anodic reaction (iron dissolution) was unaffected or rapidly retarded with increasing HAc concentration at room temperature. Guo et al (2005) studied the effect of HAc and Ac^- at 50 C, 1 bar CO_2, and 100 C, 10 bar CO_2. The polarization curves result

shows an increased cathodic currents, and indication of inhibition of the anodic reaction with increasing HAc concentration of 0-360 ppm. Galacia et al (2006) developed computer models to calculate downhole pH in presence of CO_2 and organic acids.

3. Methods and Procedure

The main samples examined in this work were machined from commercial rods of X65 mild steel with a composition of 0.08%C, 0.25% Si, and 1.54%Mn. The average chemical composition of the material is listed in Table 1. In each experiment, the specimen surfaces were polished sequentially with 80, 120, 240, 320, 600, 800, and 1200 grit SiC paper, degreased with acetone, rinsed with distilled water or ethanol, and then dried. All experiments in this study were conducted using artificial seawater (3.5% wt. NaCl) solutions saturated with CO_2. This solution mimics typical seawater found in the oilfield environment, with the composition shown in Table 2. The fresh solutions were prepared using sodium chloride from LLK Laboratories Ltd and distilled water. Table 2 presents the test matrix used for the experiments. Each test was performed in a 1-liter glass cell and at a partial pressure of 0.54 bar. Additionally, before each test, the solution in the test cell was continuously purged with CO_2 for at least 2 hours and then bubbled throughout the test to ensure complete removal of oxygen from the system.

The electrochemical measurement (EIS) was performed using a three-electrode system, with a commercially available ACM Gill AC 930 Potentiostat/galvanostat controlled by a computer. The reference electrode was Ag/AgCl, and the auxiliary electrode was a platinum electrode. The Electrochemical impedance spectroscope (EIS) measurement was used to determine the corrosion rate at a scan rate of 0.1667 mV/s.

Table 1 Chemical composition of mild steel used in this study

Chemical Composition	Values (%)
C	0.08
Si	0.25
Mn	1.54
S	0.001
P	0.019
Sn	0.008
Cr	0.04
Ni	0.03
MO	0.01
Cu	0.12
Al	0.038

Table 2 Experimental Matrix for the Electrochemical Test

Parameters	Values
Test material	Mild steel X 65 grade.
Test solution	3.5% wt. NaCl
Temperature, ^oC	[25, 50 and 80]
$p_{CO2, bar}$	0.54
HAc Conc, ppm	[0, 500, 1000, 2500]
MEG Conc, %	[20, 80]
Inhibitors Conc, ppm	[3, 5 and 10]

Test duration, hrs	6
Measurement technique	EIS
Potential ramp :	-5 to +5 mV vs. E_{corr}
sweep rate :	0.1 mV/s
EIS	5KHz – 0.01 Hz.

4. Results and Discussions

In electrochemistry, the linear polarization resistance (LPR) reflects only changes in the dissolution of the steel surface under specific conditions. Conversely, electrochemical impedance spectroscopies (EIS) is used as an alternative measurement to explain the mechanisms of electrochemical reactions that may occur at the metal-electrolyte interface. In this study, EIS was employed to demonstrate the effect of acetic acid on CO_2 corrosion of carbon steel samples in a 3.5% wt. NaCl solution. The impedance spectra were recorded at the OCP and within the frequency range of 5 kHz to 0.01 Hz, with an alternating current amplitude of ± 5 mV.The results obtained are presented.

4.1. Electrochemical Impedance Spectroscope Results with HAc

Figures 1 **Error! Reference source not found.**to 6 present the Nyquist and Bode experimental curves measured on the mild steel coupons in a CO_2 -saturated environment at various conditions.

It is observed (Figures 1 to 6) that a large capacitive semi-circle at high frequencies is seen in the absence of HAc, which is considered the capacitance of double electrode layer between the electrode and the solution. When various concentrations of HAc are added to the solution, the high-frequency semi-circle decreases in size, indicating an increase in corrosion rate and a decrease in the protectiveness of the $FeCO_3$ layer that could have formed. From the Bode plots (Figures 2, 4, and 6), the regions with high frequencies are regarded as more porous media with little or no protective layer.

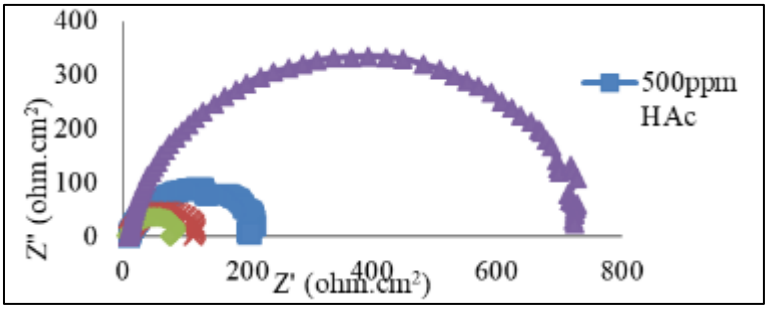

Figure 1 Nyquist plots for mild steel samples in solutions of HAc at 25 ℃ after 6 hours

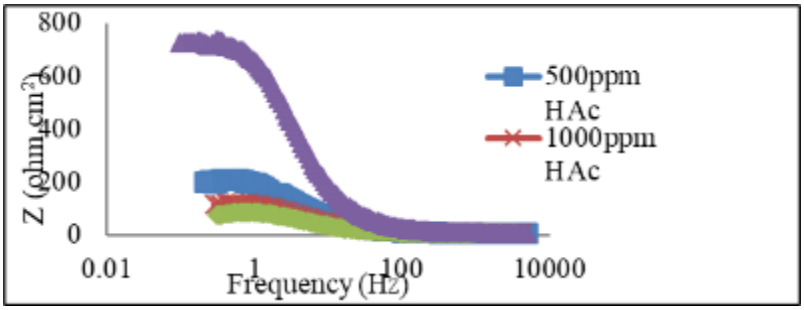

Figure 2 Bode plots for mild steel samples in solutions of HAc at 25 ℃ after 6 hours

Conversely, the low-frequency regions are less porous, where the formation of a protective layer is possible. If the protective layers are completely impaired, the corrosion is controlled by a diffusion transfer process, whereas it is a charge transfer process when the protective layer becomes more porous at the electrode-electrolyte interface. Validate the results from the Nyquist and Bode plots; an equivalent circuit model diagram in Figure 7 was used to interpret the

data. In Figure 7, Rs represents the solution resistance, C_{dl} is the double layer capacitance, and R_t is the capacitive double layer. Tables 1 to 3 summarizes the data obtained from the equivalent circuit diagram under different conditions.

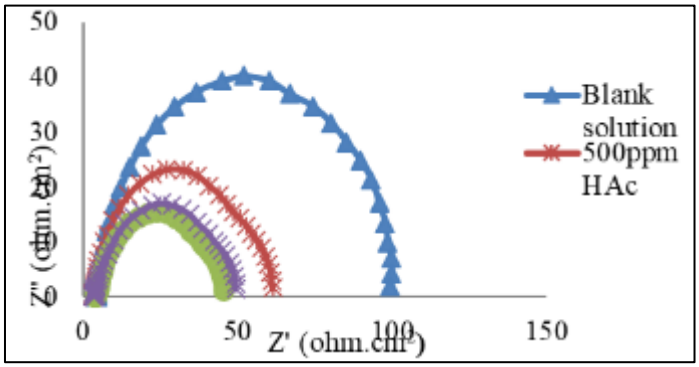

Figure 3 Nyquist plots for mild steel samples in solutions of HAc at 50 ℃ after 6 hours

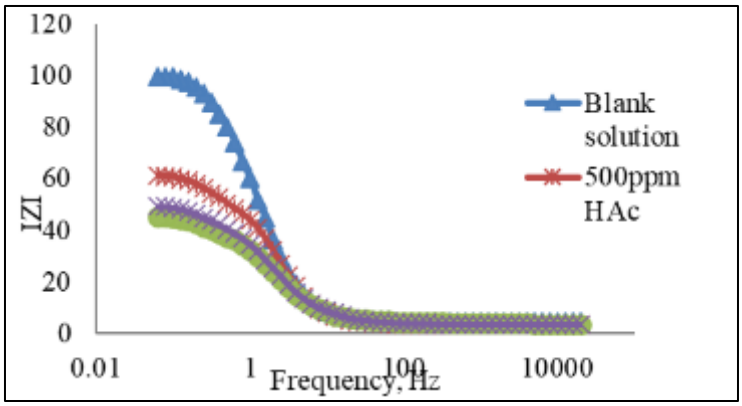

Figure 4 Bode plots for mild steel samples in solutions of HAc at 50 ℃ after 6 hours

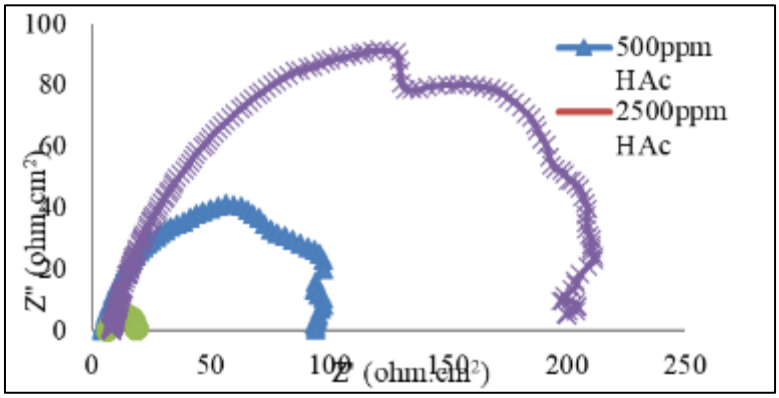

Figure 5 Nyquist plots for mild steel samples in solutions of HAc at 80 ℃ after 6 hours

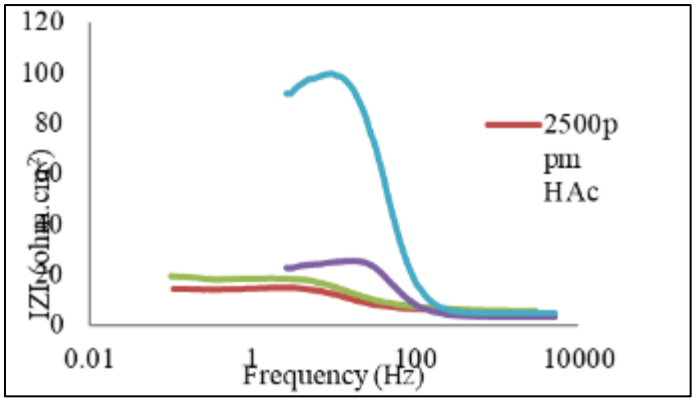

Figure 6 Bode plots for mild steel samples in solutions of HAc at 80 ℃ after 6 hours.

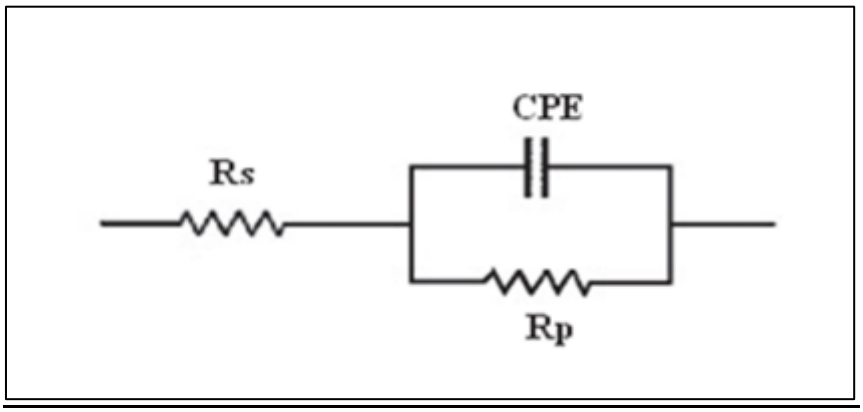

Figure 2 Equivalent circuit diagram used to fit the EIS data

Table 3 Electrochemical parameters obtained for steel electrode in solutions HAc at 25 ℃

Conc(ppm)	R_{ct} (Ω.cm²)	Rsol (Ω.cm²)	C_{dl} (µF)	Θ (°)
0	1.90	7.87	1.58	5.18
500	9.53	8.04	3.80	10.4
1000	6.97	6.62	1.12	8.4
2500	7.14	9.14	7.53	3.25
ε (%)	0.03	0.05	0.01	0.04

Table 4 Electrochemical parameters obtained for mild steel electrode in solutions HAc at 50 ℃

Conc (ppm)	R_{ct} (Ω.cm²)	Rsol(Ω.cm²)	C_{dl} (µF)	Θ (°)
0	2.87	3.22	4.15	6.75
500	3.07	4.11	5.99	3.30
1000	3.14	5.05	6.23	5.81
2500	3.38	6.64	7.58	7.33
ε (%)	0.02	0.01	0.01	0.05

Table 5 Electrochemical parameters obtained for mild steel electrode in solutions HAc at 80 °C

Conc (ppm)	R_{ct} (Ω.cm²)	Rsol (Ω.cm²)	C_{dl} (µF)	Θ (°)
0	8.36	4.24	3.58	7.61
500	9.53	4.92	2.14	7.6
1000	9.01	5.76	1.01	10
2500	1.32	5.83	1.15	9.52
ε (%)	0.02	0.01	0.03	0.04

4.2. Electrochemical Impedance Spectroscope Results with HAc and MEG

The EIS measurements were used to assess the behavior of MEG and HAc on carbon steel electrodes immersed in a 3.5% wt. NaCl solution at different temperatures. The percentage of MEG added to the solution was 20% MEG (rich MEG) and 80% MEG (lean MEG).

Figures 8 to 13 depict the Nyquist and Bode plots of the EIS measurements under various conditions. At lower temperatures (Figures 8 and 9), the Nyquist plots show a large capacitive semicircle at very high frequencies which signifies high solution resistance for the blank solution. The impedance value of the blank solution is significantly smaller compared to the impedance values with 20% and 80% MEG solutions. When 20% MEG and 80% MEG are added to the solution, the capacitance semi-circles are depressed, indicating a charge transfer process is occuring. The depressed semicircle is characteristic of frequency dispersion and has been reported by (Ueda et al, 2005) for different physical phenomenon such as surface roughness and in-homogeneities, which occur during corrosion. According to the equivalent circuit diagram for modelling and calculations (Figure 7), the solution resistance for the blank solution is approximately 8.1 ohms-cm². The addition of 20% MEG and 80% MEG increases the solution resistance to 9.20 ohms-cm² and 11.30 ohms-cm², respectively.

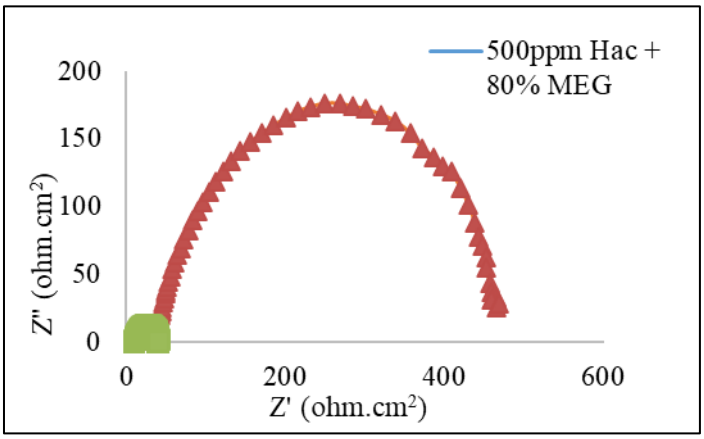

Figure 8 Nyquist plots for mild steel coupons in 3.5% wt. NaCl solution of HAc with 20% MEG and 80% MEG after 6 hours at 25 °C

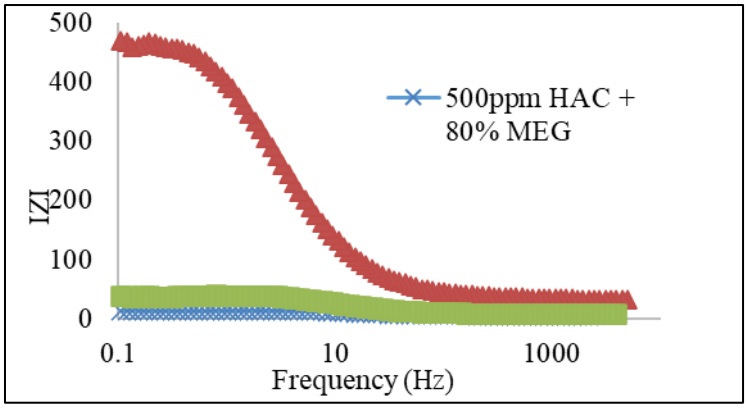

Figure 3 Bode plots for mild steel coupons in 3.5% wt. NaCl solution of HAc with 20% MEG and 80% MEG after 6 hours tests at 25 °C

The Nyquist and Bode plots for mild steel summerged in 3.5% wt. NaCl solution at various concentrations of HAc and MEG at 50 C are presented in Figures 10 and 11. It is observed that adding 20% MEG and 80% MEG results in higher solution resistance at lower temperatures. The solution resistance for the blank solution at 50 C is 9.44 ohms-cm^2 compared to 8.1 ohms-cm^2 at 25 C. With 20% MEG and 80% MEG, the solution resistance increases to 10.2 ohms-cm^2 and 16.0 ohms-cm^2 respectively. Also, it was observed that the impedance values for the solution with HAc and the blank solutions are insignificant. Both 20% MEG and 80% MEG exhibit higher impedance values, indicating that the corrosion resistance of mild steel is greater in 3.5% wt. NaCl solutions and solutions containing HAc.

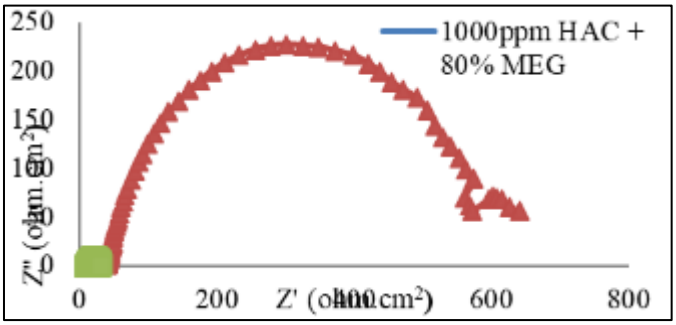

Figure 4 Nyquist plots for mild steel coupons in 3.5% wt. NaCl solution of HAc with 20% MEG and 80% MEG after 6 hours at 50 °C

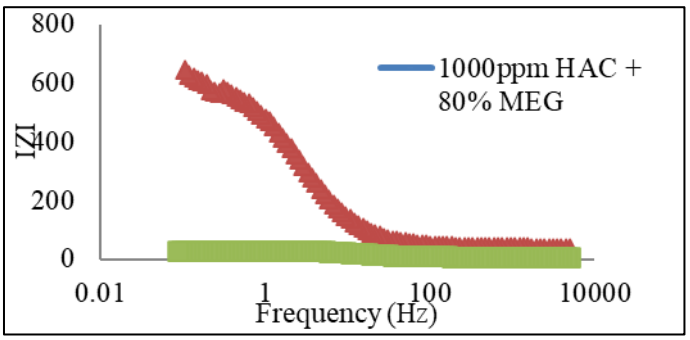

Figure 5 Bode plots for mild steel coupons in 3.5% wt. NaCl solution of HAc with 20% MEG and 80% MEG after 6 hours tests at 50 °C.

The Nyquist and Bode plots obtained from the EIS for mild steel coupons in 3.5% wt. NaCl solution in the presence of HAc and MEG at higher temperature(80 C) are presented in Figures 12 and 13, respectively. The trend of the plots indicates that the size of the Nyquist and Bode plots decreased significantly upon addition of 20% MEG and 80% MEG compared to the Nyquist plots in the presence of HAc and the blank solution. The results signify changes in the corrosion mechanisms due to the added MEG, which reduces the corrosion rates. Higher impedance indicates a higher corrosion rate at elevated temperatures. The addition of 20% MEG and 80% MEG reduces the capacitance semi-circles, which is a function of MEG concentrations. This shows that the double-layer capacitance and charge transfer resistance are indicators of corrosion inhibition. Tables 4 to 6 summarizes the parameters obtained from fitting the electrochemical impedance measurements using the equivalent circuit diagram in Figure 7.

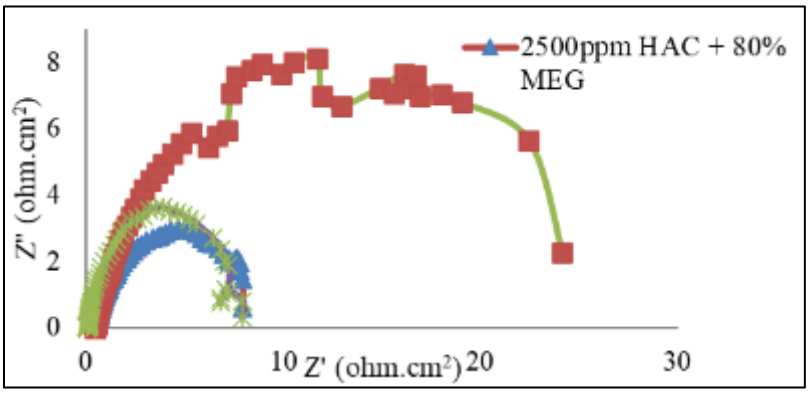

Figure 6 Nyquist plots for mild steel coupons in 3.5% wt. NaCl solution of HAc with 20% MEG and 80% MEG after 6 hours at 80 °C

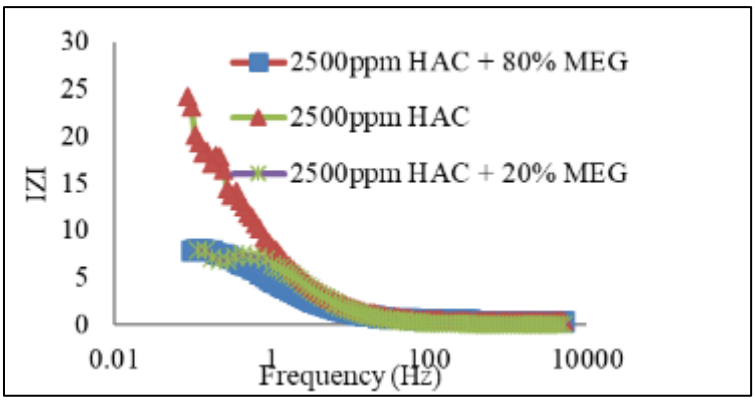

Figure 7 Bode plots for mild steel coupons in 3.5% wt. NaCl solution of HAc with 20% MEG and 80% MEG after 6 hours tests at 80 °C

Table 6 Electrochemical parameters obtained for mild steel electrode in 3.5% wt. NaCl solutions different concentrations of HAc with 20% MEG and 80% MEG at 25 °C

Composition	R_{ct} (Ω.cm²)	Rsol (Ω.cm²)	C_{dl} (F)	Θ (°)
Solution + 20% MEG + 0ppm HAc	35	8.1	197	0
Solution + 20% MEG + 500ppm HAc	64	9.20	69	65
Solution + 20% MEG + 1000ppm HAc	109	11,3	77	61
Solution + 20% MEG + 2500ppm HAc	210	10.21	34	83
Solution + 80% MEG + 0ppm HAc	48	13.6	22	89
Solution + 80% MEG + 500ppm HAc	76	12.9	56	72

Solution + 80% MEG + 1000ppm HAc	112	10.15	40	80
Solution + 80% MEG + 2500ppm HAc	230	11.8	76	61
(%) ε	±0.02	±0.05	±0.01	±0.02

Table 7 Electrochemical parameters obtained for mild steel electrode in 3.5% wt. NaCl solutions of different concentrations of HAc with 20% MEG and 80% MEG at 50 °C

Composition	**R_{ct} ($\Omega.cm^2$)**	**R_{sol} ($\Omega.cm^2$)**	**C_{dl} (F)**	**Θ (°)**
Solution + 20% MEG + 0ppm HAc	57	9.44	146	26
Solution + 20% MEG + 500ppm HAc	75	16.0	80	59
Solution + 20% MEG + 1000ppm HAc	130	10.2	34	83
Solution + 20% MEG + 2500ppm HAc	240	11.8	54	73
Solution + 80% MEG + 0ppm HAc	65	9.05	60	70
Solution + 80% MEG + 500ppm HAc	77	9.95	39	80
Solution + 80% MEG + 1000ppm HAc	120	11	50	75
Solution + 80% MEG + 2500ppm HAc	248	10.2	57	71
(%)ε	±0.03	±0.04	±0.02	0±.02

4.3. Electrochemical Impedance Spectroscope Results with HAc, MEG and Inhibitors

Figures 14 to 19 show a typical EIS Nyquist and Bode plots of carbon steel in 3.5% wt. NaCl solution obtained in this study. The curves feature one depressed semi-circle at high frequencies and another at lower frequencies. The depressed semi-circle at high frequencies indicates low solution conductivity, which causes the solution resistance between the reference electrode and the working electrode in the presence of inhibitors. At lower frequencies, the depressed semi-circle reflects the due to carbon steel corrosion process in the solution.

In Figures 14 to 19, it is observed that a depressed capacitive semi-circle appears at high frequency for the solution with inhibitors compared to the blank solution at low frequency, and an inductive semi-circle is also seen. The depressed capacitive semi-circle results from the of time constant of the electric double layer and the charge transfer resistance of the solution. The depressed inductive semi-circle observed at low frequency is due to adsorption relaxation of intermediates. The presence of a single depressed semi-circle indicates that the corrosion inhibitors slow down the acceleration of the corrosion process during the dissolution of carbon steel.

At 25 C (Figures 14 and 15) the size of the depressed semi-circle of Nyquist plots on application of inhibitors XX and YY is almost the same compared to the size of inhibitor ZZ though with one single depressed semi-circle. These trends implies that almost the same inhibition mechanisms occur during the dissolution of carbon steel samples in the solution. It was also noticed that the impedance plots consist of a single capacitance loop at very high frequency.

Adding of different concentrations of inhibitors to solutions with 20% MEG and 80% MEG and HAc increased the capacitance of depressed semi-circles, which is linked to the double layer capacitance and charge transfer resistance that slow down the corrosion process. A decrease in the depressed semicircle was also seen in the Nyquist plots when inhibitor YY was applied. This indicates that the corrosion process with inhibitor YY is controlled more by charge transfer rather than activation.

In order to obtain useful information from the corrosion process, such as the corrosion rate, the EIS data was analyzed using an equivalent circuit diagram of elements shown in Figure 7.

Table 8 Electrochemical parameters obtained for mild steel electrode in 3.5% wt. NaCl solutions of different concentrations of HAc with 20% MEG and 80% MEG at 80 ℃

Composition	**R_{ct} ($\Omega.cm^2$)**	**Rsol ($\Omega.cm^2$)**	**C_{dl} (F)**	**Θ (°)**
Solution + 20% MEG + 0ppm HAc	45	7.5	130	34
Solution + 20% MEG + 500ppm HAc	66	9.08	55	72
Solution + 20% MEG + 1000ppm HAc	125	11.2	44	78
Solution + 20% MEG + 2500ppm HAc	208	10.65	56	72
Solution + 80% MEG + 0ppm HAc	58	11.5	64	68
Solution + 80% MEG + 500ppm HAc	65	9.8	40	80
Solution + 80% MEG + 1000ppm HAc	109	12	65	67
Solution + 80% MEG + 2500ppm HAc	221	10.5	70	64
ε (%)	0.02	0.05	0.03	0.01

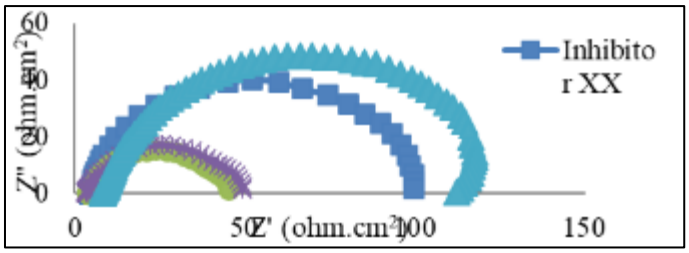

Figure 14 Nyquist plots for mild steel coupons in 3.5% wt. NaCl solution of HAc, 20% MEG, 80% MEG, and corrosion inhibitors for 6 hours at 25 ℃

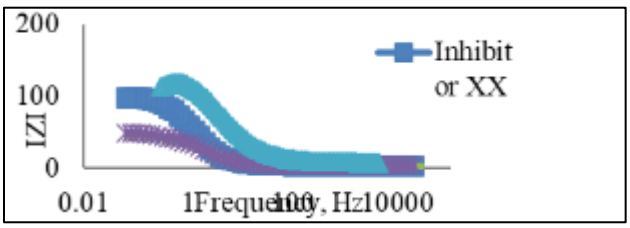

Figure 8 Bode plots for mild steel coupons in 3.5% wt. NaCl solution of HAc, 20% MEG, 80% MEG, and corrosion inhibitors for 6 hours at 25 ℃

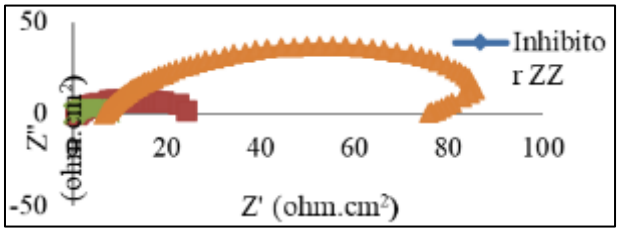

Figure 9 Nyquist plots for mild steel coupons in 3.5% wt. NaCl solution of HAc, 20% MEG, 80% MEG, and corrosion inhibitors for 6 hours at 50 ℃

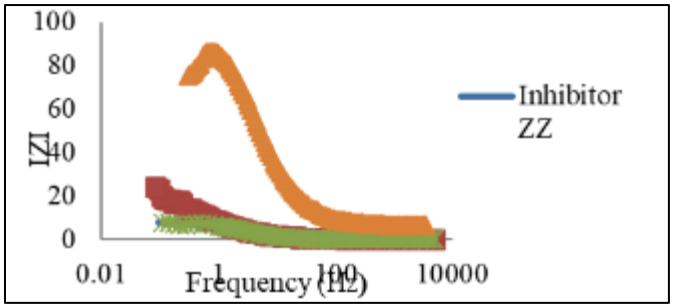

Figure 10 Bode plots for mild steel coupons in 3.5% wt. NaCl solution of HAc, 20% MEG, 80% MEG, and corrosion inhibitors for 6 hours at 50 ℃

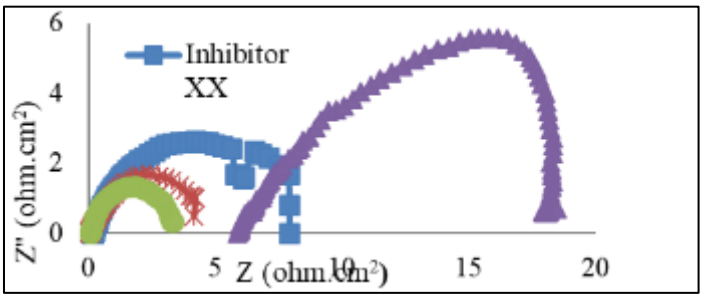

Figure 11 Nyquist plots for mild steel coupons in 3.5% wt. NaCl solution of HAc, 20% MEG, 80% MEG, and corrosion inhibitors for 6 hours at 80 ℃

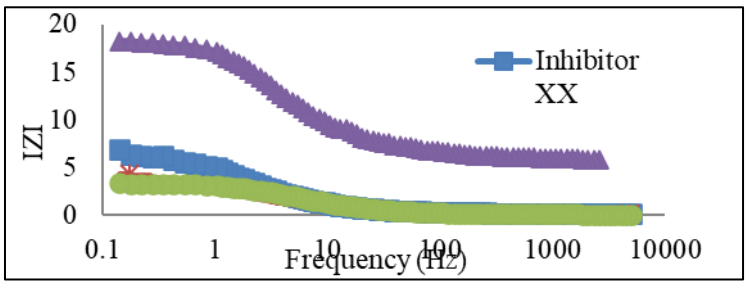

Figure 12 Bode plots for mild steel coupons in 3.5% wt. NaCl solution of HAc, 20% MEG, 80% MEG, and corrosion inhibitors for 6 hours at 80 ℃

5. Conclusions

The experimental studies oo the synergistic effects of HAc and MEG on the corrosion of mild steel in a CO_2 -saturated environment at different temperatures of 25 ℃, 50 ℃ and 80 ℃, with a pH of 6.6, and a CO_2 partial pressure of 0.54 bar, have been conducted.. Additionally, the inhibitive performance of three organic corrosion inhibitors (XX, YY, and ZZ) on CO_2-induced corrosion of carbon steel in 3.5% wt NaCl solutions containing acetic acid and mono-ethylene glycol was also evaluated. Electrochemical measurements using an electrochemical impedance spectroscope are employed to determine the relationship between the corrosion rate and corrosion potential over of time. Based on this study and the results obtained so far, the following conclusions are made.

- It is demonstrated that the addition of rich MEG and Lean MEG (20% MEG and 80% MEG), along with a 3.5% wt. NaCl solution, reduces the corrosion rate at all temperatures compared to when only HAc is present. The results observed with the addition of 20% and 80% MEG show that there are changes in the mechanism of CO2 corrosion of carbon steel, due to the of prevention of reaction sites by the addition of 20% MEG and subsequently slowing down the corrosion reaction at high concentrations (80%) of MEG.
- The electrochemical measurements have shown that the corrosion rate increases with higher concentrations of HAc, and decreases with longer exposure times. This is due to the formation of an iron carbonate film on the surface of the steel sample.

- The effectiveness of the organic corrosion inhibitor studied in 3.5% wt NaCl solution was confirmed by the EIS results obtained. However, it was noted that inhibition efficiency increases with the inhibitor concentration. Similarly, the analysis of the equivalent circuit diagram revealed that increasing the inhibitor concentration from 3 ppm to 10 ppm decreased the circuit capacitance and increased the polarization resistance at the electrode-electrolyte interface.
- The three corrosion inhibitors examined have proven to effectively prevent mild steel corrosion in a CO2-saturated environment. It was observed that their inhibition efficiency increases with concentration, reaching about 75% at a concentration of 10 ppm.
- The use of corrosion inhibitors in all tested conditions further decreases the corrosion rate to its lowest level. All three inhibitors tested showed satisfactory inhibition performance at concentration ranging from 3 ppm to 10 ppm, compared to samples without inhibitors.
- Finally, the Bode and Nyquist plots of the EIS measurement showed that the diameter of the depressed semicircle decreased as the concentrations of HAc and MEG increased, and the sizes of the capacitive semicircle also shrank with the addition of 20% and 80% MEG to 3.5% NaCl solutions containing HAc.

Compliance with ethical standards

Acknowledgement

The authors would like to express their appreciation to the technical staff at the University of Salford, Manchester, and the Department of Petroleum and Gas Engineering at the University of Port Harcourt for their support throughout this work.

Disclosure of conflict of interest

The authors declare no conflict of interest.

References

[1] Abayarathna, D., A. Naraghi, and N. Obeyesekere, Inhibition of Corrosion of Carbon Steel in the Presence of CO2, H2S and S. NACE International.

[2] Andersen, T.R., et al., The Influence Of Condensation Rate And Acetic Acid Concentration On Tol-Corrosion In Multiphase Pipelines. 2007, NACE International.

[3] Bardal, E., Corrosion and Protection. 2004: Springer.

[4] Bonis, M.R. and J.L. Crolet, Why So Low Free Acetic Acid Thresholds, in Sweet Corrosion at Low PCO2? NACE International.

[5] Abayarathna, D., A. Naraghi, and N. Obeyesekere, Inhibition of Corrosion of Carbon Steel in the Presence of CO2, H2S and S. NACE International.

[6] Andersen, T.R., et al., The Influence Of Condensation Rate And Acetic Acid Concentration On Tol-Corrosion In Multiphase Pipelines. 2007, NACE International.

[7] Bardal, E., Corrosion and Protection. 2004: Springer.

[8] Bonis, M.R. and J.L. Crolet, Why So Low Free Acetic Acid Thresholds, in Sweet Corrosion at Low PCO2? NACE International.

[9] Brustad, S., K.P. Løken, and J.G. Waalmann, Hydrate Prevention using MEG instead of MeOH: Impact of experience from major Norwegian developments on technology selection for injection and recovery of MEG. Offshore Technology Conference.

[10] Burgan, B.A., S.C. Institute, and S.S.A. Centre, Concise Guide to the Structural Design of Stainless Steel. 1993: Steel Construction Institute.

[11] C.A Barlow, J., The Electrical Double Layer in physical chemistry: An Advanced Treatise, in Electrochemistry. 1970, Academic press, New York.

[12] Charng, T.L., F., Review of corrosion causes and corrosion control in a technical facility. 1982: United States.

[13] Chechirlian, S., et al., A specific aspect of impedance measurements in low conductivity media. Artefacts and their interpretations. Electrochimica Acta, 1990. 35(7): p. 1125-1131.

[14] Cottis, R.A., Lecture notes on Corrosion. University of Manchester, Corrosion and Protection Center, 2009.

[15] Crolet, J.L., N. Thevenot, and A. Dugstad, Role of Free Acetic Acid on the CO2 Corrosion of Steels. NACE International.

[16] Dugstad, A., M. Seiersten, and R. Nyborg, Flow Assurance of pH Stabilized Wet Gas Pipelines. NACE International.

[17] G.H.Koch, M.P.H.B., N.G.Thompson,Y.P.Virmani, and J.H.Payer, Corrosion Cost and Preventon Strategies in the United States. Federal highway administration, U.S. Department of Transportation: McLean VA., 2002.

[18] G1-03, A., Standard Practice for Preparing, Cleaning, and Evaluating Corrosion Test Specimens. ASTM International, West Conshohocken, PA, 2011, www.astm.org, 2011.

[19] Garsany, Y., D. Pletcher, and B.M. Hedges, The Role of Acetate in CO2 Corrosion of Carbon Steel: Has the Chemistry Been Forgotten? NACE International.

[20] George, K.S. and S. Nešić, Investigation of Carbon Dioxide Corrosion of Mild Steel in the Presence of Acetic Acid—Part 1: Basic Mechanisms. CORROSION, 2007. 63(2): p. 178-186.

[21] Gulbrandsen, E., Acetic Acid And Carbon Dioxide Corrosion Of Carbon Steel Covered With Iron Carbonate. NACE International.

[22] Gunaltun, Y. and L. Payne, A New Technique for the Control of Top of the Line Corrosion: TLCC-PIG. NACE International.

[23] Guo, S., F. Farelas, and M. Singer, Effect of Monoethylene Glycol on Sweet Top of the line corrosion. NACE International.

[24] Guo, X.P., et al., Novel quantitative method for evaluation pitting corrosion and pitting corrosion inhibition of carbon steel using electrochemical noise analysis. Journal of Materials Science, 2005. 40(17): p. 4469-4473.

[25] Halvorsen, A.M. and T. Sontvedt, CO2 Corrosion Model for Carbon Steel Including Wall Shear Stress Model for Multiphase Flow and Limits for Production Rate to Avoid Mesa Attack. NACE International.

[26] Hassan, H.H., E. Abdelghani, and M.A. Amin, Inhibition of mild steel corrosion in hydrochloric acid solution by triazole derivatives: Part I. Polarization and EIS studies. Electrochimica Acta, 2007. 52(22): p. 6359-6366.

[27] Hedges, B. and L. McVeigh, The Role of Acetate in CO2 Corrosion: The Double Whammy. NACE International.

[28] Hurlen, T., et al., Corrosion and passive behaviour of aluminium in weakly acid solution. Electrochimica Acta, 1984. 29(5): p. 579-585.

[29] Kermani, M.B. and A. Morshed, Carbon Dioxide Corrosion in Oil and Gas Production—A Compendium. CORROSION, 2003. 59(8): p. 659-683.

[30] Kermani, M.B. and D. Harrop, The Impact of Corrosion on Oil and Gas Industry.

[31] Lindsay, R. and S.B. Lyon, 4.25 - Introduction to Control of Corrosion by Environmental Modification, in Shreir's Corrosion. 2010, Elsevier: Oxford. p. 2891-2899.

[32] Lu, H., A.T. Kan, and M.B. Tomson, Effects of Monoethylene Glycol on Carbonate Equilibrium and Calcite Solubility in Gas/Monoethylene Glycol/Water/Salt Mixed Systems. Society of Petroleum Engineers.

[33] Mendez, C., et al., On the Mechanism of Corrosion Inhibition by Crude Oils. NACE International.

[34] Nafday, O. and S. Nesic, Iron Carbonate Scale Formation and CO2 Corrosion in the Presence of Acetic Acid. NACE International.

[35] Nešić, S., Key issues related to modelling of internal corrosion of oil and gas pipelines–A review. Corrosion science, 2007. 49(12): p. 4308-4338.

[36] Oblonsky, L.J., M.P. Ryan, and H.S. Isaacs, In situ determination of the composition of surface films formed on Fe-Cr alloys. JOURNAL OF THE ELECTROCHEMICAL SOCIETY, 1998. 145: p. 1922-1932.

[37] Okafor, P.C., B. Brown, and S. Nesic, CO2 corrosion of carbon steel in the presence of acetic acid at higher temperatures. Journal of Applied Electrochemistry, 2009. 39(6): p. 873-877.

[38] Perez, T.E., Corrosion in the Oil and Gas Industry: An Increasing Challenge for Materials. JOM, 2013. 65(8): p. 1033-1042.

[39] Pojtanabuntoeng, T., M. Salasi, and R. Gubner, The Influence of Mono Ethylene Glycol (MEG) on CO2 Corrosion of Carbon Steel at Elevated Temperatures (80 to 120oc). NACE International.

[40] Qiu, J.H. and P.H. Chua, EIS and XPS study of the corrosion of carbon steel in inhibited natural seawater. Surface and Interface Analysis, 1999. 28(1): p. 119-122.

[41] Roberge, P.R., Corrosion basics: An introduction. 2006, NACE Press Book. p. 56-70.

[42] S.Nesic, J.P.a., Erosion–Corrosion in Single- and Multiphase Flow. 2011, in Uhlig's Corrosion Handbook: John Wiley & Sons, Inc., Hoboken, NJ, USA. .

[43] Singer, M., et al., Combined effect of carbon dioxide, hydrogen sulfide, and acetic acid on bottom-of-the-line corrosion. Corrosion, 2011. 67(1).

[44] Smart, J., A review of erosion corrosion in oil and gas production. J. S. Smart, III. CORROSION 90/10, NACE, Houston, TX. Per Copy$, 1990.

[45] Sun, Y., K. George, and S. Nesic, The Effect of Cl- and Acetic Acid on Localized CO2 Corrosion in Wet Gas Flow. NACE International.

[46] Ueda, M. and H. Takabe, Effect of Organic Acid on CO2 Corrosion of Carbon and CR Bearing Steels. NACE International.

[47] Videm, K., "Fundamental Studies aimed at Improving Models for Prediction of CO2 Corrosion", Progress in the Understanding and Prevention of Corrosion. Institute of Metals,, London, 1993.

[48] Waard, C.d., U. Lotz, and D.E. Milliams, Predictive Model for CO2 Corrosion Engineering in Wet Natural Gas Pipelines. CORROSION, 1991. 4**7**(12): p. 976-985.

[49] Wang, C., et al., Corrosion Study of Carbon Steel in the Presence of Monoethylene Glycol (MEG) and Corrosion Inhibitors in Acid. NACE International.

[50] Zhang, Q., et al., Corrosion behavior of Hastelloy C-276 in supercritical water. Corrosion Science, 2009. 51(9): p. 2092-2097.

[51] Brustad, S., K.P. Løken, and J.G. Waalmann, Hydrate Prevention using MEG instead of MeOH: Impact of experience from major Norwegian developments on technology selection for injection and recovery of MEG. Offshore Technology Conference.

[52] Burgan, B.A., S.C. Institute, and S.S.A. Centre, Concise Guide to the Structural Design of Stainless Steel. 1993: Steel Construction Institute.

[53] C.A Barlow, J., The Electrical Double Layer in physical chemistry: An Advanced Treatise, in Electrochemistry. 1970, Academic press, New York.

[54] Videm, K., "Fundamental Studies aimed at Improving Models for Prediction of CO2 Corrosion", Progress in the Understanding and Prevention of Corrosion. Institute of Metals,, London, 1993.

[55] WAARD, C.D. and D.E. MILLIAMS, Carbonic Acid Corrosion of Steel. CORROSION, 1975. **31**(5): p. 177-181.

[56] Waard, C.d., U. Lotz, and D.E. Milliams, Predictive Model for CO2 Corrosion Engineering in Wet Natural Gas Pipelines. CORROSION, 1991. 4**7**(12): p. 976-985.

[57] Wang, C., et al., Corrosion Study of Carbon Steel in the Presence of Monoethylene Glycol (MEG) and Corrosion Inhibitors in Acid. NACE International.

[58] Wang, H., et al., Characterization of Inhibitor and Corrosion Product Film Using Electrochemical Impedance Spectroscopy (EIS). NACE International.

[59] Xianghong, L., et al., Inhibition of the corrosion of cold rolled steel in hydrochloric acid solution by Tween-40. Anti-Corrosion Methods and Materials, 2009. 56(4): p. 232-238.

[60] Yong Xiang, M.Y., Yoon-Seok Choi, David Young, Srdjan Nesic, Time-dependent electrochemical behaviour of carbon steel in MEA. International Journal of Greenhouse Gas Control, 2014. 30: p. 125-132.

[61] Zhang, Q., et al., Corrosion behavior of Hastelloy C-276 in supercritical water. Corrosion Science, 2009. 51(9): p. 2092-2097.

[62] Zhang, Y., et al., Modeling steel corrosion under supercritical CO2 conditions. Materials and Corrosion, 2013. 64(6): p. 478-485.